International Journal of Pharmaceutics 414 (2011) 161–170

Contents lists available at ScienceDirect

International Journal of Pharmaceutics

journal homepage: www.elsevier.com/locate/ijpharm

Doxorubicin and paclitaxel loaded microbubbles for ultrasound triggered drug delivery

Michael C. Cochran [a], John Eisenbrey [a], Richard O. Ouma [a], Michael Soulen [b,c], Margaret A. Wheatley [a,*]

[a] School of Biomedical Engineering Science and Health Systems, Drexel University, Philadelphia, PA 19104, United States
[b] Division of Interventional Radiology, University of Pennsylvania, PA, United States
[c] Department of Radiology, University of Pennsylvania, PA, United States

ARTICLE INFO

Article history:
Received 9 February 2011
Received in revised form 15 April 2011
Accepted 6 May 2011
Available online 13 May 2011

Keywords:
Ultrasound contrast agent
Microbubble
Paclitaxel
Nanoparticle
Targeted drug delivery

ABSTRACT

A polymer ultrasound contrast agent (UCA) developed in our lab has been shown to greatly reduce in size when exposed to ultrasound, resulting in nanoparticles less than 400 nm in diameter capable of escaping the leaky vasculature of a tumor to provide a sustained release of drug. Previous studies with the hydrophilic drug doxorubicin (DOX) demonstrated enhanced drug delivery to tumors when triggered with ultrasound. However the therapeutic potential has been limited due to the relatively low payload of DOX. This study compares the effects of loading the hydrophobic drug paclitaxel (PTX) on the agent's acoustic properties, drug payload, tumoricidal activity, and the ability to deliver drugs through 400 nm pores. A maximum payload of 129.46 ± 1.80 μg PTX/mg UCA (encapsulation efficiency $71.92 \pm 0.99\%$) was achieved, 20 times greater than the maximum payload of DOX (6.2 μg/mg), while maintaining the acoustic properties. In vitro, the tumoricidal activity of paclitaxel loaded UCA exposed to ultrasound was significantly greater than controls not exposed to ultrasound ($p < 0.0016$). This study has shown that PTX loaded UCA triggered with focused ultrasound have the potential to provide a targeted and sustained delivery of drug to tumors.

1. Introduction

Recent interest in ultrasound assisted drug delivery has focused attention on active drug targeting (Price et al., 1998; Ferrara et al., 2007; Ferrara, 2008). In addition, passive targetting through use of nanoparticles continues to be advanced (Panyam and Labhasetwar, 2003; Fang et al., 2011), especially with drugs which are particularly toxic or troublesome to deliver, such as paclitaxel. Paclitaxel (PTX) is an antineoplastic agent that promotes the polymerization of tubulin and at subnanomolar concentrations, can inhibit the disassembly of microtubules (Rowinsky and Donehower, 1995). This disruption of normal microtubule dynamics can inhibit cell proliferation and cause cell death (Yeung et al., 1999). Paclitaxel has shown significant activity against solid tumors including breast cancer and ovarian carcinomas (Thigpen et al., 1994; Ishitobi et al., 2001; Conlin and Seidman, 2007). Breast cancer is the most common form of cancer diagnosed in women (Jemal et al., 2008). Taxanes including PTX have proven to be fundamental in the treatment of early-stage and advanced forms of breast cancer. The effects of paclitaxel on breast cancer cell lines including the MDA-MB 231 and MCF 7 human breast cancer cell line have been well studied and have been used to confirm the tumoricidal activity of novel drug delivery formulations in vitro (Yeung et al., 1999; Rosenblum and Shivers, 2000; Kang et al., 2004). The use of this drug has been limited by its poor aqueous solubility (Liggins et al., 1997), requiring use of an excipient, Cremophor®. Methods to mitigate the adverse effects of this excipient include the use of micro and nanoparticles, micelles and lipid based contrast agents (Green et al., 2006; Tartis et al., 2006; Li and Wallace, 2008; Miele et al., 2009; Gaucher et al., 2010; Klibanov et al., 2010). Systemic delivery of Taxol can cause severe side effects including hypersensitivity reactions (Weiss et al., 1990; Gelderblom et al., 2001) neurotoxicity, cardiotoxicity and neutropenia (Rowinsky and Donehower, 1995). A variety of alternative strategies including micelles, liposomes, microspheres and nanoparticles are being investigated to deliver PTX without the use of Cremophor® (Singla et al., 2002). Nanoparticles fabricated with albumin (Ibrahim et al., 2002) poly lactic-co glycolic acid (PLGA) (Mu and Feng, 2003) and poly lactic acid (PLA) (Xie and Wang, 2005) have been loaded with PTX and used to passively target tumors (Hamaguchi et al., 2005). Abraxane®, an albumin bound nanoparticle formulation of PTX, has been created as a Cremophor® free delivery vehicle of PTX that has been shown to be superior to standard PTX in the treatment of breast cancer (Miele et al., 2009).

Passive targeting of tumors is based on the enhanced permeability and retention (EPR) effect. Most solid tumors are sustained

* Corresponding author. Tel.: +1 215 895 2232; fax: +1 215 895 4983.
E-mail address: wheatley@coe.drexel.edu (M.A. Wheatley).

0378-5173/$ – see front matter © 2011 Elsevier B.V. All rights reserved.
doi:10.1016/j.ijpharm.2011.05.030

by extensive angiogenesis leading to hypervascular tissue with an incomplete vascular architecture. Tumors also have an impaired lymphatic drainage and an increased production of permeability factors resulting in the accumulation and inefficient clearance of nanoparticles leading to the EPR effect (Maeda et al., 2000). The hyperpermeable nature of tumor vasculature is characterized by a pore cut off size ranging between 380 and 780 nm allowing particles less than 780 nm to extravasate into the tumor interstitium (Hobbs et al., 1998).

The vascular permeability of tumors can be enhanced with the use of specific growth factors (Dvorak et al., 1995), hyperthermia (Kong et al., 2000), or through the use of ultrasound contrast agents (UCA) combined with targeted ultrasound (Price et al., 1998). Ultrasound contrast agents (UCA) are small (<6 μm) gas bubbles encapsulated within a stabilizing shell. When exposed to the oscillating pressures of an ultrasound wave, the gas core of a UCA will rapidly expand and contract with a wall velocity on the order of hundreds of meters per second (Ferrara et al., 2007). When exposed to sufficient ultrasound intensity, UCA can cavitate, resulting in enough energy to temporarily increase the permeability of the capillary wall, allowing particles to escape the vessel and travel tens of microns into the interstitium (Ferrara, 2008).

In addition to their role in increasing vascular permeability and enhancing drug uptake within tumors, lipid and polymer shelled UCA have themselves been loaded with drugs (Ferrara et al., 2009; Eisenbrey et al., 2010a). The polymer shelled UCA developed in this lab have been loaded with doxorubicin (DOX) and when exposed to ultrasound have been shown to rupture, creating drug-loaded polymer fragments, 350 nm in size, capable of accumulating within a tumor and slowly releasing drug (Eisenbrey et al., 2010b). This in situ generation of nanoparticles at the tumor site from circulating bubbles utilizes the strong, size-dependent interaction between ultrasound and micron-sized particles, such as acoustic radiation forces and microstreaming (Lum et al., 2006; Ferrara, 2008), combined with the abilities of nanoparticles to escape the tumor vasculature and provide a sustained release of drug. This platform combines the advantages of ultrasound assisted drug delivery with the use of traditional, passively targeted (through EPR) nanoparticles. We have tested a DOX–UCA in vivo in a rabbit tumor model and were able to demonstrate a 110% increase in drug delivery to the tumor when exposed to ultrasound, compared to uninsonated controls (Eisenbrey et al., 2010b). However, the maximum DOX payload of this agent was found to be only 6.2 μg DOX/mg UCA with an encapsulation efficiency of 20.5% (Eisenbrey et al., 2010a), making achieving therapeutic concentrations difficult.

This paper focuses on comparing the loading of DOX with that of the more hydrophobic drug PTX within the shell of these biodegradable UCA and characterizing the agent in vitro as a prelude to in vivo testing. PTX is an ideal candidate for this type of drug delivery since it would be delivered directly to the tumor site and the need for toxic excipients such as Cremophor® EL would be avoided. Maximum drug loading was determined, along with the effects of drug loading on the agent's acoustic enhancement, acoustic stability and size. The drug release profile of UCA exposed to ultrasound was compared with uninsonated UCA and the in vitro tumoricidal activity of the PTX loaded agent was examined.

2. Materials and methods

2.1. Materials

Poly(lactic acid) (PLA) (100DL MW = 83 kDa) was purchased from Lakeshore Biomaterials (Birmingham, AL). Camphor, DOX used for in vitro experiments, and thiazolyl blue tetrazolium bromide (MTT) were purchased from Sigma–Aldrich (St. Louis, MO). Radiolabeled DOX (labeled with a 14C linker as part of a previous study [Eisenbrey et al., 2010b]) used for in vivo experiments was purchased from Perkin Elmer (Waltham, MA). Poly(vinyl alcohol) (PVA) (88% mole hydrolyzed MW = 25 kDa) was purchased from Polysciences (Warrington, PA). Paclitaxel was purchased from LC Laboratories (Woburn, MA). CellTracker Blue was purchased from Molecular Probes (Carlsbad, CA). All other chemicals were reagent grade from Fisher Scientific (Waltham, MA). All chemicals were used as received.

2.2. Sample preparation

Doxorubicin and PTX loaded UCA were prepared with a water in oil in water emulsion technique based on a method previously developed in our laboratory (El-Sherif and Wheatley, 2003). A solution with 0.05 g of camphor, 0.5 g of PLA with 3.0% DOX (the point of drug payload saturation [Eisenbrey et al., 2010a]) or varying amounts of PTX 0–24% (weight PTX/weight PLA) were dissolved in 10 ml of methylene chloride. To form the first emulsion, 1 ml of ammonium carbonate (4%, w/v) was added to the polymer solution and sonicated in an ice water bath with 110 W of applied power with ten pulses of 3 s separated by 1 s pauses using a 20 kHz sonicator probe (Misonix Inc. CL4 tapped horn probe with a 0.5 in. tip Farmingdale, NY). The second emulsion was formed by adding the first water in oil emulsion to 50 ml of a cold PVA solution (5%, w/v) then homogenizing for 5 min at 9500 rpm with a saw tooth homogenizer blade (Brinkmann Instruments, Westbury, NY). After homogenizing, 100 ml of 2% isopropyl alcohol was added to the emulsion then stirred for 1 h at room temperature to allow the methylene chloride to evaporate. The resulting suspension was centrifuged at 2500 × *g* for 5 min. The supernatant was discarded and the pellet was washed three times with hexane. After allowing residual hexane to evaporate the samples were washed with water three times, then frozen in liquid nitrogen and lyophilized for 48 h with a Virtis Benchtop freeze dryer (Gardiner, NY) to allow the water, camphor and ammonium carbonate to sublimate, resulting in a hollow core surrounded by a porous PLA, drug-loaded shell containing PTX.

2.3. In vitro acoustic testing

The ability of UCA samples to reflect ultrasound was determined with an in vitro acoustic setup. A 5 MHz, 0.5 in. diameter transducer (Panametrics-NDT Waltham, MA) with a focal length of 45 mm and a −6 dB bandwidth of 89.3% was chosen in order to insonate the samples with a frequency that closely matched the resonance frequency of this UCA. The transducer was placed in a 37 °C water bath and focused through the acoustically transparent window of an acrylic sample holder containing 50 ml of 37 °C phosphate buffered saline, pH = 7.4 (PBS). The transducer was connected to a pulser/receiver (Panametrics Waltham, MA) to generate an acoustic pulse with a pulse repetition frequency (PRF) of 100 Hz and a peak negative pressure amplitude of 0.45 MPa measured with a 0.5 mm polyvinylidene fluoride needle hydrophone (Precision Acoustics, Dorset, UK). The reflected signal was detected with the transducer and amplified 40 dB by the pulser/receiver then displayed by an oscilloscope (Lecroy 9350 A Chestnut Ridge, NY). Labview 7 Express (National Instruments, Austin, TX) was used for data acquisition and processing.

Acoustic backscattering enhancement was used to measure the agent's ability to respond to ultrasound for imaging and drug delivery applications. Dry samples of UCA were weighed and suspended in PBS then pipetted into the buffer in the sample holder and allowed to mix for 10 s before measuring the acoustic response at

the focus of the transducer. Acoustic backscattering enhancement was defined as:

$$\text{Enhancement} = 20 \log \left(\frac{\text{rms[UCA]}}{\text{rms[Blank]}} \right)$$

where rms[UCA] is the root mean square of the backscatter signal given by the UCA at the focus of the transducer, and rms[Blank] is the root mean square of the backscatter signal given by the solution prior to the addition of UCA.

The acoustic stability of UCA exposed to ultrasound was measured to determine the effect of drug loading on shell stability. Three microgram of UCA per milliliter of PBS was added to the sample holder and insonated continuously with a PRF of 100 Hz and a peak negative pressure amplitude of 0.45 MPa. Acoustic enhancement was measured every minute over the course of 15 min and normalized with respect to the initial enhancement.

2.4. Particle sizing

The sizes of UCA were measured using a Zetasizer Nano ZS (Malvern Inst., Worcestershire, UK). One milligram of dry UCA was carefully weighed and suspended in 1 ml of PBS by vortexing for 10 s. Samples were measured in triplicate and particle sizes were reported as peak % number. Number was chosen since this more clearly represents an emphasis on populations of smaller size (which from scanning electron microscopy data dominate here). Volume values are overly sensitive to a few large volume particles.

2.5. Determination of drug loading

The amount of PTX loaded into the UCA was determined in triplicate by high pressure liquid chromatography (HPLC). Two milligrams of UCA were dissolved in 1 ml of methylene chloride. The PTX was then extracted into 3 ml of an acetonitrile/water solution (50:50, v/v) and the methylene chloride was allowed to evaporate. For HPLC analysis, a reverse-phase Inertsil ODS-3 column (150 × 3 mm i.d., pore size 5 μm GL Sciences, Tokyo, Japan) was used. The mobile phase of acetonitrile/water (50:50, v/v) was delivered at a flow rate 1 ml/min (Waters 1525 binary pump, Milford, MA) and PTX was quantified by UV absorbance (λ = 227 nm, Waters 2487 Milford, MA). The area under the curve was integrated and the PTX concentration was calculated based on a linear calibration curve. Encapsulation efficiency was defined as:

$$\text{Encapsulation efficiency (\%)} = \frac{\text{Amount of drug in UCA (μg)}}{\text{Initial amount of drug (μg)}} \times 100$$

2.6. In vivo ultrasound imaging

In vivo imaging was performed in a VX2 liver cancer model implanted in New Zealand rabbits to determine ultrasound enhancement and the agent's ability to permeate the vasculature of a tumor model. Rabbits were anesthetized using ketamine (35 mg/kg), xylazine (2 mg/kg), and glycopyrolate (0.01 mg/kg). After sedation, 2–3 mm cubes of VX2 tumor harvested from the thigh of a carrier rabbit were implanted into the left lobe of the liver. Tumors were then allowed to grow for 3 weeks, reaching sizes of roughly 2–3 cm^3. Animals were housed in accordance with the Guide for the Care and Use of Laboratory Animals. All animal studies described here were performed in accordance with the guidelines of the Institutional Animal Care and Use Committee of the University of Pennsylvania.

Rabbits received an injection of 70 mg of agent (containing 2 mg DOX) suspended in 5 ml of physiological saline through an auricular line, then flushed with an additional 5 ml of saline. Tumors were continually insonated for 20 min by non-directional Doppler ultrasound focused on the tumor (ATL/Philips HDI-5000, Bothel, WA). Ultrasound was performed at 5 MHz, PRF = 1000 Hz, frame rate = 10 Hz and the transducer: L12-5 38 generic probe, with a MI of 1.0 and continually swept over the tumor. Videos were then stored and digitized for later use.

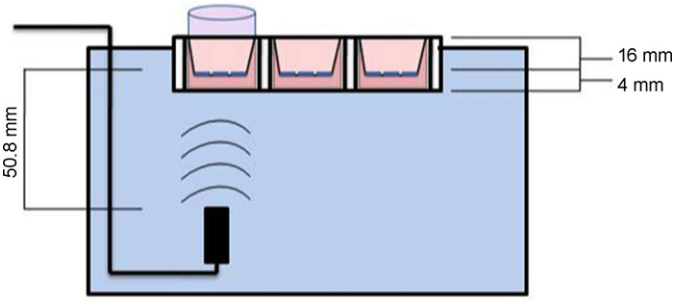

Fig. 1. Diagram of transwell insert/well plate assembly combined with ultrasound setup. A pulser/receiver is used to generate acoustic pressure amplitudes vertically using the transducer, focused 50.8 mm on the cell/pore membrane.

Time–intensity curves were computed in Matlab (Version 2009a, The Mathworks, Natick, MA). Digitized clips at a frame rate of 10 Hz were imported as single frames. Image intensity in arbitrary units (a.u.) was then calculated by the summation of pixel intensity within the tumor ROI at each time point. A 10 point moving average was then applied to reduce noise in the intensity curve before being plotted as a function of time.

2.7. In vitro PTX release

Drug loaded UCA loaded with 18% PTX were suspended in PBS at 37 °C with a concentration of 0.2 mg/ml and placed into the acoustic sample holder described above with stirring. The previously described acoustic setup was used to insonate the UCA with a peak negative pressure amplitude of 0.94 MPa and a PRF of 5000 Hz for 25 min. Controls were performed with no insonation. Ten milliliters of the suspension was then transferred to centrifuge tubes and incubated at 37 °C while being rotated end over end. At selected time intervals the samples were centrifuged at 48,000 × *g* for 20 min (Sorvall WX ultracentrifuge, AH-629 rotor, Thermo Electron Corp., Waltham, MA). The amount of PTX released from the particles at every time point was less than the solubility of PTX (Liggins et al., 1997). The pellet was resuspended in fresh PBS at each time interval (to maintain sink conditions) and placed in the incubator to continue the release. At no point did the PTX concentration in the release buffer approach saturated values. The collected supernatants were extracted two times with 1 ml of methylene chloride. The extracted methylene chloride was allowed to evaporate and the PTX was dissolved in 1 ml of running buffer. The extraction efficiency was calculated in triplicate using 10 ml solutions with known concentrations of PTX in PBS and put through the same extraction procedure.

2.8. Nanoparticle extravasation potential

The ability of PTX loaded UCA to fragment in response to ultrasound and pass through the leaky vasculature of a tumor was modeled in vitro with Corning Transwell® inserts (Corning Incorporated, Corning, NY) with a polyester membrane containing 400 nm pores (Fig. 1). The inserts were placed in polystyrene 6 well plates containing 3 ml of PBS at 37 °C containing 1 mg PTX loaded UCA. The insert was then filled with 1 ml of PBS at 37 °C and a rubber stopper was placed at the upper level of the PBS in the insert to act as an acoustic absorber and reduce reflections at the air–liquid interface that may lead to a standing wave. The plate was then

held at the surface of the water in a 37 °C water bath with a 5 MHz transducer focused on the membrane of the insert from below. The sample was insonated for 20 min with a peak negative pressure of 0.94 MPa and a PRF of 5000 Hz. Samples were taken immediately prior to insonation and at 5 min intervals. Paclitaxel levels were quantified with HPLC as described previously. Tests were repeated in triplicate, controls were performed without insonation.

2.9. Cell culture

The human breast cancer cell lines MDA-MB-231 and MCF7 were obtained from American Type Culture Collection (Manassas, VA). MDA-MB-231 cells (passage 6) were cultured to 70% confluency within Opticell® culture systems (Fisher Scientific, Springfield, NJ) in media containing 94% RPMI 1640, 5% FBS, and 1% penicillin/streptomycin antibiotic. MCF7 cells were grown in RPMI 1640 medium, supplemented with 10% (v/v) FBS and 1% (v/v) antibiotic. Cells were maintained in a humidified incubator at 37 °C in a 5% CO_2 atmosphere.

2.10. Cellular uptake of PLA–DOX shards after insonation

The ability of drug loaded UCA to provide targeted delivery of drug into cells when triggered with ultrasound was tested in vitro using DOX loaded UCA in order to take advantage of the natural fluorescence of DOX for drug tracking. MDA-MB-231 cells were grown to 70–80% confluency within Opticell® culture systems. After removal of medium, 6 mg of 3% DOX–UCA in 10 ml of medium was added and the Opticells® insonated at a peak negative pressure of 0.94 MPa. Cells were incubated in solution for 12 h to allow uptake and reattachment before the cell medium was removed and cells washed twice with PBS. Cell cytoplasm was then stained using CellTracker Blue stain and fixed within the Opticell® with 4% paraformaldehyde prior to imaging. Uninsonated cells incubated with 6 mg of 3% loaded DOX–UCA in 10 ml of medium were used as a control. Fluorescent confocal microscopy was performed on cells 12 h after insonation to identify the location of DOX within the cell and the results presented as merged images of fluorescent and bright field.

Confocal imaging was performed using an Olympus IX81 microscope run by Olympus Fluorview version 1.7b. The CellTracker Blue cytoplasm dye was visualized with 405/461 nm excitation/emission wavelengths. DOX was simultaneously imaged by using wavelength of 488/578 nm excitation and emission. Proper gain levels were determined automatically using the Fluorview software.

2.11. In vitro tumoricidal activity

Cells were seeded on 48 well plates with a density of 2.5×10^4 cells per well in 500 μl of media and incubated overnight to allow cells to attach. Ultrasound contrast agents with 0% and 18% PTX (weight PTX/weight PLA) were insonated in media for 20 min with a peak negative pressure of 0.94 MPa and a PRF of 5000 Hz. After insonation, the samples were filtered through 0.45 μm filters to simulate leaky tumor vasculature and allow only nanoparticles to pass through. The samples were then diluted in media and added to the attached cells. Controls were performed without insonation. Cells were incubated with the treatment for 72 h and tumoricidal activity was evaluated with an MTT assay. Culture media was removed and cells were washed with PBS then incubated with 500 μl of the MTT solution (0.5 mg MTT/ml serum free RPMI) for 3 h at 37 °C. The solution was then removed and 1 ml of an acidic isopropyl alcohol solution (isopropyl alcohol – 0.04 M HCl) was used to dissolve the formazan crystals. Absorbance of the solution was measured at 570 nm with a Tecan Infinite M200 plate reader (Männedorf, Switzerland). Cells without MTT were used as a blank to calibrate the measurements and untreated cells were used as controls. Cell viability was calculated with the following equation:

$$\text{Cell viability } (\%) = \frac{\text{Absorbance (sample)}}{\text{Absorbance (untreated control)}} \times 100$$

2.12. Scanning electron microscopy

Contrast agent was imaged using an environmental SEM (FEI XL30, Hillsboro, OR, USA). A freeze dried sample mounted on a stub with two sided carbon tape was sputter-coated with platinum for 30 s before imaging. Images were taken at varying magnifications, with an accelerating voltage of 10.0 kV. All SEM imaging was done at the Drexel University Materials Characterization Facility.

2.13. Statistical analysis

Statistical differences for multiple groups were determined using a one way ANOVA and individual groups were compared using Student's *t*-test. All statistical testing was done with Prisim (GraphPad, San Diego, CA). Statistical significance was determined using $\alpha = 0.05$, values are represented as an average with a standard error about the mean.

3. Results

3.1. Proof of principle in DOX–UCA

3.1.1. Visualization of ultrasound damage

Previously we have shown that the PLA UCA developed in our lab can be loaded with drug (Eisenbrey et al., 2010a), shattered into nano sized particles with ultrasound (Eisenbrey et al., 2010b) and cause cell death in vitro (Eisenbrey et al., 2009). Fig. 2 shows scanning electron micrographs of drug loaded capsules after fabrication and after insonation in vitro at for 20 mins at 5 MHz at an peak negative pressure of 0.94 MPa. While the pre-insonated agent shows mainly intact, spherical particles, the insonated particles show clear signs of destruction. These destroyed particles appear to consist of both ruptured and shriveled particles, as well as a new population of nanoparticle shell fragments. We have extended these studies in vitro to track the fate of the particles in cell culture.

3.1.2. In vitro fate of particles

To investigate the possible fate of nanoshards in contact with cells, we tracked DOX–UCA nano shards in vitro. Fig. 3 compares the fluorescent image of MDB-MA 231 cells grown in culture and treated with DOX–UCA in the presence and absence of ultrasound. DOX fluorescence is clearly concentrated within the nucleus, indicating that after ultrasound triggering DOX appears in the cytoplasm of the cell, but also in the nucleus where it can trigger cell death.

3.1.3. In vivo penetration into tumor vasculature

In vivo imaging was conducted showing the agent's potential to both provide enhancement during ultrasound scans, and penetrate into the vasculature of a solid tumor. Doppler ultrasound was used to image the solid tumor at a frequency of 5 MHz at a MI of 1.0, corresponding to estimated pressures above what have been shown to cause destruction of polymer shelled UCA (Bloch et al., 2004), ensuring maximal UCA rupture and fragment generation. Fig. 4 shows Doppler images of the tumor pre and post injection of the UCA. Fig. 4a shows the VX2 tumor prior to the UCA arrival, with little Doppler signal in the tumor. Fig. 4b is an image of the same tumor at the point of peak contrast enhancement (48 s after injection) presumably due to peak drug carrier concentrations within the tumor. By 66 s carrier washout is well underway (Fig. 4c).

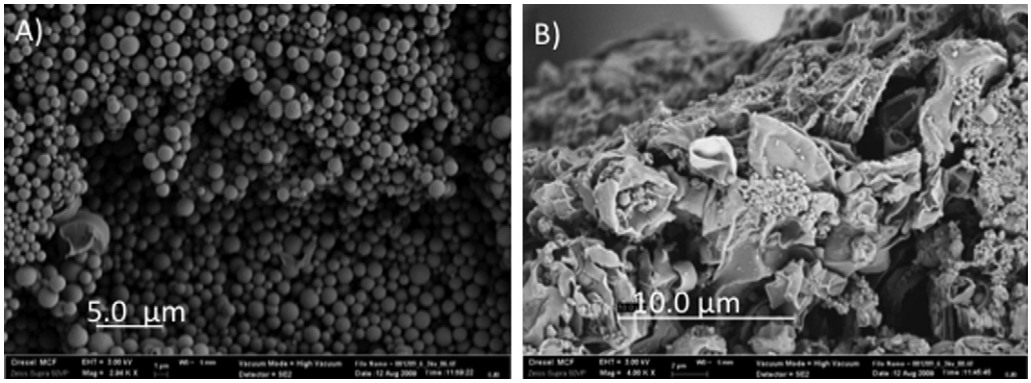

Fig. 2. DOX loaded UCA, (a) prior to insonation. Samples shows a smooth surface morphology and average diameter of 1.2–1.6 μm (accelerating voltage = 3 kV, magnification = 2.94k×, size bar = 5 μm. (b) After resuspension in buffer, 20 min insonation at 5 MHz, 0.94 MPa, and freeze drying. Insonation results in shell rupture and generation of DOX loaded nanoparticles (accelerating voltage = 3 kV, magnification = 4.00k×, size bar = 10 μm).

The washout process can be recorded in time–intensity curves in arbitrary units (a.u.), an example of which is given in Fig. 4d. Fluctuations in the curve are due to the animal breathing and sweeping by the transducer.

These images show that the UCA penetrates into the solid tumor. For drug release studies in vivo, the ultrasound beam can be focused entirely on the solid tumor (1–2 cm^2 surface area), initiating destruction of UCA within this region.

3.2. In vitro acoustic enhancement and stability of PTX–UCA

The effect of PTX loading on the agent's acoustic properties was examined using an acoustic testing setup developed in our lab for UCA characterization (El-Sherif and Wheatley, 2003). Fig. 5a shows the effect of PTX loading on the acoustic behavior of the agent and the impact of loading on the ability to reflect ultrasound as measured by acoustic enhancement in decibels (dB) compared to enhancement in the absence of agent. Paclitaxel loading did not result in any significant differences in maximum acoustic enhancement compared to unloaded control UCA ($p > 0.076$), however UCA loaded with 12% PTX or greater did show significantly more shadowing at a dose of 15 μg/ml compared to unloaded controls ($p < 0.0058$).

Effects of PTX loading on the agent's acoustic stability during insonation were also measured and are shown in Fig. 5b.

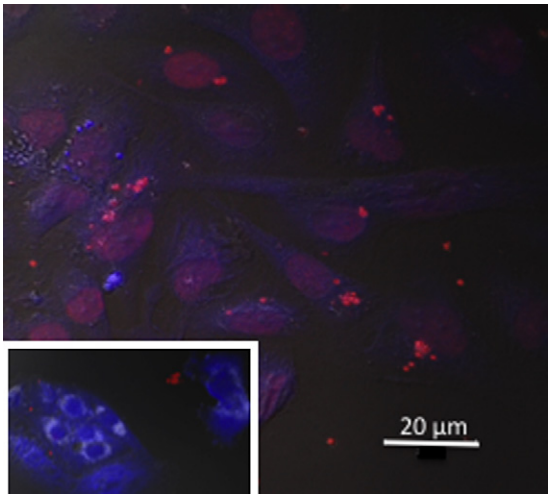

Fig. 3. Confocal image of MDA-MB-231 cells @12 h after 5 MHz insonation with DOX–UCA (3%) at a peak negative pressure of 0.94 MPa. Inset no treatment (size bar = 20 μm).

The enhancement in dB decreased with time as the agent passed through the ultrasound beam and was destroyed. Unloaded UCA maintained 78% of their initial enhancement after 15 min, while UCA loaded with 3% PTX or more, maintained significantly less enhancement ($p < 0.034$) less than 70% of their original enhancement after 15 min.

3.3. Particle size

The effect of PTX loading concentration on UCA size was examined (Fig. 6). Particles were loaded with initial concentrations up to 6% PTX (with particle sizes of 1383 ± 59 nm, 1610 ± 127 nm and 1737 ± 146 nm corresponding to a PTX loading of 0, 3 and 6%) without any significant difference in particle size compared to unloaded control particles ($p > 0.0653$), although an increasing size trend was evident. However, particles loaded with 12% PTX or greater showed a significant increase in particle size compared to unloaded UCA ($p < 0.0197$ with particle sizes of 1864 ± 127 nm, 2021 ± 194 nm and 2833 ± 337 nm corresponding to a PTX loading of 12, 18 and 24%).

3.4. Paclitaxel payload and encapsulation efficiency

Paclitaxel encapsulation was quantified with HPLC and is shown in Fig. 7a over a range of loading concentrations, along with the encapsulation efficiency shown in Fig. 7b. Final drug payload increased significantly with each increase in initial loading concentration up to 18% PTX ($p < 0.001$) while particles loaded with the highest initial loading concentration of 24% PTX did not have a significantly greater final payload compared to particles loaded with 18% PTX (131.12 ± 10.94 μg PTX/mg PLA vs. 129.46 ± 1.80 μg PTX/mg PLA, $p = 0.8807$). The encapsulation efficiency of UCA loaded with 3, 6 and 12% PTX were approximately 75% and were not significantly different from each other. However the increase in loading from 12 to 18% PTX resulted in a significantly lower encapsulation efficiency ($84.52. \pm 1.48\%$ vs. $71.92 \pm 0.99\%$, $p = 0.0021$) and the encapsulation efficiency of particles loaded with 18% PTX was significantly greater than particles loaded with 24% PTX ($71.92 \pm 0.99\%$ vs. $54.68 \pm 4.55\%$, $p = 0.0209$). An initial loading of 18% PTX was selected as the optimal loading percentage for future experiments.

3.5. In vitro paclitaxel release

The release profiles of PTX loaded UCA exposed to ultrasound and uninsonated controls were examined in vitro using capsules loaded with 18% PTX (Fig. 8). After 48 h there was no significant difference in the percentage of total PTX released from insonated and

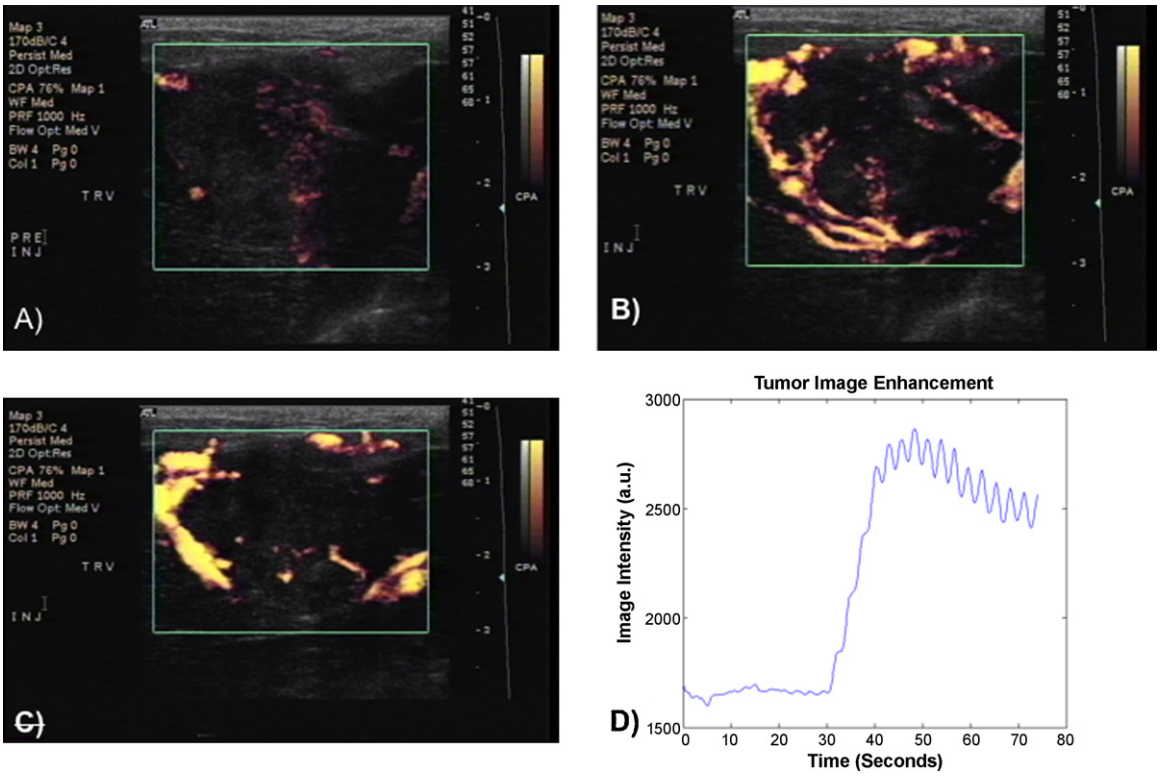

Fig. 4. Enhancement of VX2 liver tumor model during stages of drug delivery. At 22 s, rabbits were injected with UCA. (a) Prior to the UCA arrival, (b) the same tumor at the point of peak contrast enhancement (48 s), (c) carrier washout (66 s). (d) Representative time–intensity curve in arbitrary units (a.u.) of this washout process. Fluctuations in the curve are due to the animal breathing and sweeping by the transducer.

uninsonated UCA ($24.76 \pm 2.59\%$ vs. $24.21 \pm 2.87\%$, $p = 0.8946$). After 11 days, a difference in release from UCA treated with ultrasound and controls can be observed ($41.79 \pm 2.28\%$ vs. $35.50 \pm 2.90\%$, $p = 0.16$), this difference becomes statistically significant after 21 days, when the release of PTX from insonated UCA became significantly greater than uninsonated controls ($51.66 \pm 2.45\%$ vs. $40.05 \pm 3.11\%$, $p = 0.0374$) and remained significantly greater at all additional time points.

3.6. Nanoparticle extravasation potential

Corning transwell inserts with a thin polyester membrane containing pores 400 nm in diameter were used to model the leaky tumor vasculature and to determine if delivery of PTX through the pores using PTX loaded UCA can be triggered with ultrasound. The delivery of PTX through the pores over 20 min with and without ultrasound is shown in Fig. 9. After 5 min, significantly more drug was forced through the membrane when the PTX loaded UCA were triggered with ultrasound compared to samples not exposed to ultrasound ($p = 0.0281$). After 20 min, 75% more drug (representing 11.1% of the initial drug concentration) was forced through the 400 nm pores when the agent was exposed to ultrasound compared to uninsonated controls ($p < 0.001$).

3.7. In vitro tumoricidal activity

Human breast cancer cells that were exposed to both unloaded and PTX loaded UCA that were exposed to ultrasound as well as uninsonated controls over a range of concentrations from 0 to 10 μg UCA/ml. After 72 h cell viability was measured with a MTT assay to determine the anti tumor activity of the triggered particles as shown in Fig. 10.

Unloaded UCA did not have any effect on cell viability at any concentration tested up to 10 μg/ml, both UCA exposed to ultrasound and uninsonated UCA did not reduce cell viability compared to controls ($p > 0.5465$). Ultrasound contrast agents loaded with 18% PTX triggered by ultrasound resulted in a significant increase in tumoricidal activity compared to uninsonated controls at concentrations greater than 0.1 μg UCA/ml ($p < 0.01$). The cell viability of samples treated with 1 μg/ml of PTX loaded UCA was significantly lower when triggered with ultrasound ($49.81 \pm 3.28\%$) compared to uninsonated controls ($89.69 \pm 4.09\%$) $p = 0.0016$.

4. Discussion

An alternative drug delivery platform has been developed in our laboratory in which the hydrophilic drug DOX has been loaded into the shell of polymer UCA (Eisenbrey et al., 2010a,b). Ultrasound contrast agents pass freely through the vasculature until exposed to ultrasound where they experience various interactions which push the bubbles towards the vessel wall (Lum et al., 2006) and we believe result in production of nano shards in situ at the imaged tumor site (Eisenbrey et al., 2010a,b). When exposed to sufficiently strong ultrasound pulses, the microbubble will undergo a phenomenon known as inertial cavitation (Ferrara et al., 2007; Ferrara, 2008) resulting in the destruction of the polymer shell, creating drug loaded polymer fragments less than 400 nm (Eisenbrey et al., 2010b). The energy released in the process of microbubble destruction is sufficient to enhance the permeability of the tumor vessel walls (Price et al., 1998). Any fragments that do not penetrate the tumor can then begin to accumulate within the tumor interstitium through the EPR effect (Maeda et al., 2000), and here the polymer fragments can begin to degrade providing a sustained localized release of the chemotherapeutic agent. It is therefore vital

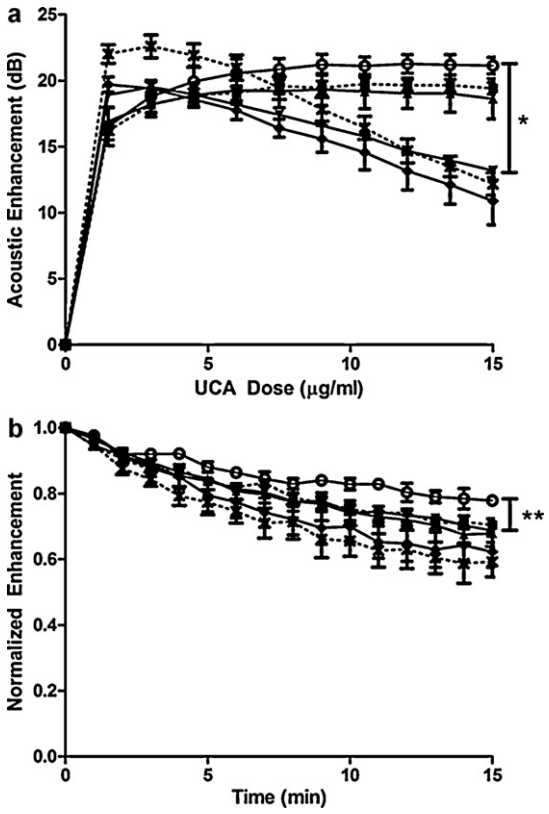

Fig. 5. Effects of PTX loading concentration on the acoustic behavior, (a) enhancement and (b) acoustic stability in vitro of UCA loaded with (0% , 3% , 6% , 12% , 18% and 24% PTX). No significant difference in maximum enhancement was observed at any loading concentration ($p > 0.076$), however samples loaded with 12% PTX or greater showed significantly more shadowing at a dose of 15 μg/ml (*$p < 0.0058$). All samples loaded with 3% PTX or greater showed significantly less stability than unloaded UCA after 15 min (**$p < 0.034$).

that our drug-loaded contrast agents retain the acoustics properties of the unloaded UCA.

Loading of DOX is limited because of its low solubility in the solvent used to create the contrast agent's polymer shell. In this work, we show SEM evidence that this DOX–UCA is fragmented by ultrasound and can deliver DOX to the nucleus, and that the agent penetrates the vasculature of a VX2 tumor in a rabbit model.

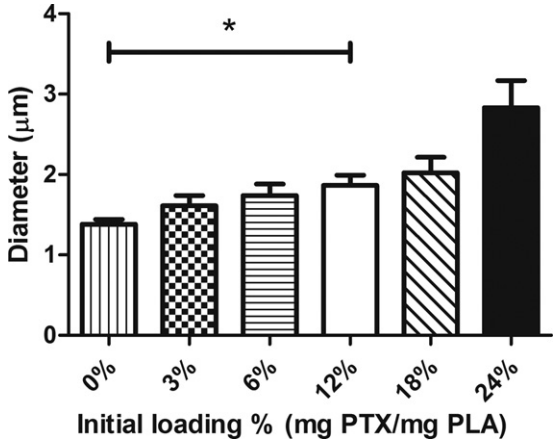

Fig. 6. Effect of PTX loading concentration on UCA size. Unloaded contrast agent had a diamter of 1.38 ± 0.12 μm, UCA loaded with 12, 18 and 24% were significantly larger ($p < 0.0197$) with diamters of 1.86 ± 0.25 μm, 2.02 ± 0.39 μm and 2.83 ± 0.67 μm respectively.

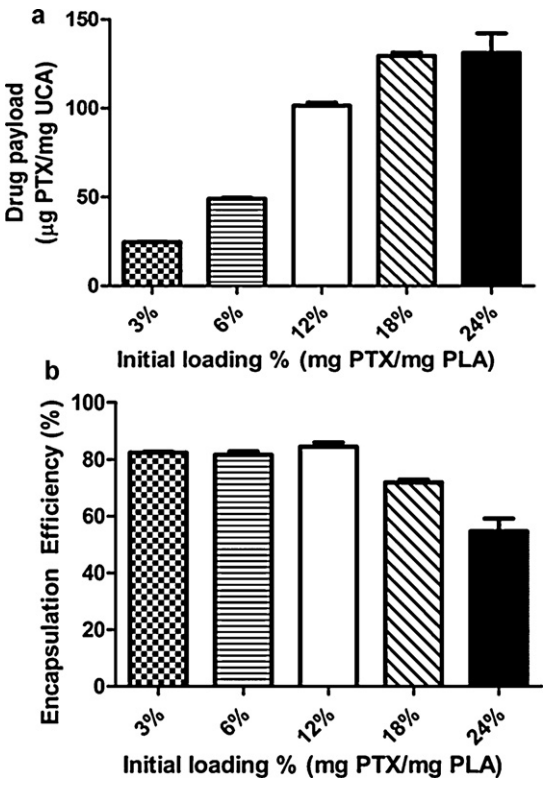

Fig. 7. Final paclitaxel payload as a function of initial loading concentration (a) and encapsulation efficiency (b). Paclitaxel loaded UCA approached their maximum payload of 129.46 μg/mg (encapsulation efficiency of 71.92%) at an initial loading concentration of 18% PTX with no significant increase in payload when the initial loading concentration was increased to 24% PTX ($p = 0.8807$).

The appearance in vitro of DOX within the nucleus of cultured cells after insonation in the presence of DOX–UCA indicates that the DOX is now in a form that is readily accessible to the cells. However, in Fig. 3 there is also a lack of DOX within the cytoplasm. This is believed to be due to the physical attraction forces between the DOX–PLA fragments and DNA, causing DOX within the cell to bind to DNA and eventually aggregate within the nucleus. Uninsonated cells showed minimal DOX within the nucleus, indicating that uptake is ultrasound dependant and we attribute this to the fact that insonation causes in situ generation of nano particles that are more prone to endocytosis and cell uptake. The phenomena of UCA delivered encapsulated DOX appearing centralized

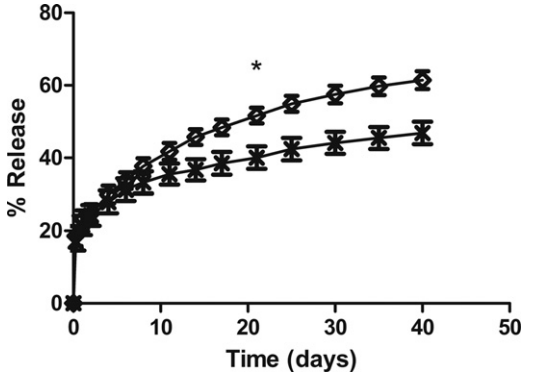

Fig. 8. In vitro drug release profile of PTX from drug loaded UCA loaded with 18% PTX exposed to ultrasound and uninsonated UCA . The release profile of insonated UCA closely matched the release of uninsonated UCA over the first week of release ($p > 0.5619$). After 21 days significantly more PTX had released from insonated UCA compared to UCA not exposed to ultrasound (*$p < 0.0374$).

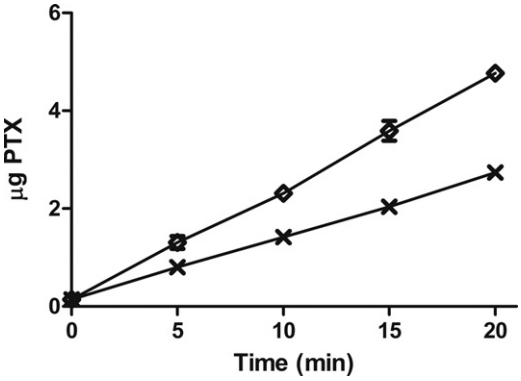

Fig. 9. Transport through membranes with 400 nm pores of PTX loaded UCA exposed to ultrasound ◆ and uninsonated UCA ✱. After 20 min of insonation, 75% more PTX was forced through the 400 nm pores than uninsonated controls ($p < 0.001$).

within the nucleus has begun to be documented in the literature, as has the importance of the drug remaining encapsulated post release. Lentacker et al. formulated DOX–liposome loaded UCA and showed increased melanoma cell nucleic uptake and cell death when insonated with 1 MHz, 50% duty cycle, ultrasound with an intensity of 2 W/cm^2 in vitro compared to DOX–liposomes alone (Lentacker et al., 2010). Additionally, several groups have shown that cells in close proximity to cavitating contrast agents become temporarily more permeable, a potential mechanism that would explain our observation of an increase of PLA–DOX shards in the cell (van Wamel et al., 2004, 2006; Meijering et al., 2009). The addition of ultrasound is also expected to lead to increased interaction between the UCA and cells as radiation forces are generated, pushing the UCA towards the cells and forcing interaction between the two. Thus, the addition of ultrasound provides a three-fold advantage for drug delivery in vitro; 1: decreased size of the particles due to UCA rupture, 2: temporarily increased permeability of the cellular membrane, and 3: increased interaction of the DOX–UCA with cells due to acoustic radiation forces.

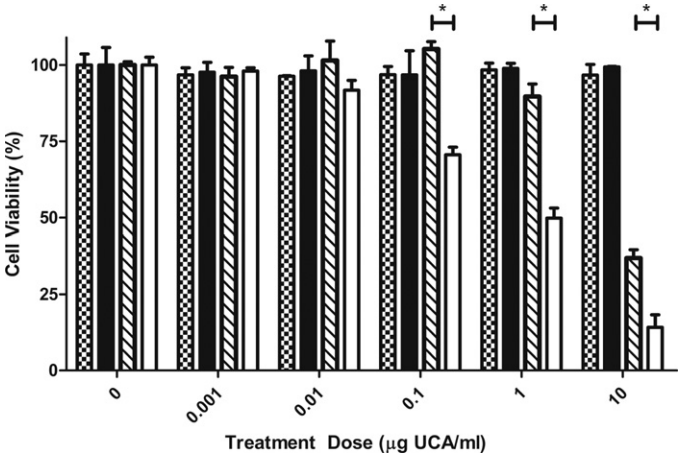

Fig. 10. Effect of treatment regime on tumoricidal activity of UCA. Samples were either not insonated (patterned) or insonated for at 5 MHz for 20 min (solid) and assayed 72 h post treatment. Unloaded UCA not exposed to ultrasound ▨, unloaded UCA exposed to ultrasound ▩, 18% PTX loaded UCA not exposed to ultrasound ■ and 18% PTX loaded UCA exposed to ultrasound □. Unloaded UCA exposed to ultrasound and uninsonated loaded UCA showed no significant decrease in cell viability at any concentrations tested ($p > 0.4827$). Ultrasound contrast agents loaded with 18% PTX and exposed to ultrasound showed significantly greater anti tumor activity at concentrations of 0.1, 1.0 and 10 μg/ml compared to uninsonated controls ($p < 0.0016$).

These results, and the fact that in a previous study tracking of radiolabeled DOX in rabbit showed an increase of 0.26 ng DOX/g tissue upon insonation, an increase of 110% in tumor drug load relative to the noninsonated control (Eisenbrey et al., 2010b), reinforce our belief that our drug loaded PLA agents can enter the tumor as nano shards where it has the capability to kill cells. However, efficacy of a DOX–UCA platform in systemic circulation is limited by its low drug payloads due to the hydrophilic nature of the drug. We now investigate a more potent, highly hydrophobic drug as a prelude to in vivo studies.

To extend this method to a more potent drug, we chose to investigate the highly hydrophobic Pactilaxel. Polymer UCA were successfully loaded with PTX without significantly reducing the agent's maximum enhancement at any loading concentrations. This indicates that the addition of such a hydrophobic drug to the shell of the microbubble does not prevent the formation of echogenic microbubbles. Microbubbles loaded with greater than 12% PTX did show significant shadowing compared to unloaded UCA (Fig. 5a). The observed increase in shadowing fits with the significant ($p < 0.0197$) increase in size of UCA loaded with greater than 12% PTX (Fig. 6). This is expected since attenuation coefficients scale with size (Gorce et al., 2000). Increase in size of the UCA as the drug loading increases probably reflect the influence of increasing organic phase viscosity and the increase in drug/polymer ratio on microcapsules prepared by the w/o/w emulsion method. The acoustic stability of UCA exposed to ultrasound was significantly reduced when the agent was loaded with PTX (Fig. 5b), a phenomenon that was also observed with DOX incorporation (Eisenbrey et al., 2010a). This decrease in stability is advantageous for the purpose of ultrasound targeted drug delivery as we intend for these PTX-loaded UCA to fragment when triggered with ultrasound and generate nano-sized fragments of drug loaded polymer (nanoshards).

Ultrasound contrast agents had a maximum PTX payload of 129.46 ± 1.80 μg PTX/mg UCA when loaded with an initial concentration of 18% PTX corresponding to an encapsulation efficiency of $71.92 \pm 0.99\%$ (Fig. 7). The maximum payload of PTX is 20 times greater than the maximum payload of DOX (6.2 μg/mg) while maintaining an encapsulation efficiency three times greater than the encapsulation efficiency of DOX (20.5%) (Eisenbrey et al., 2010a). This reflects the greater hydrophobicity of PTX, the low solubility in water and the high solubility in the organic phase of the water/oil/water emulsion. This allows the platform to carry a much greater payload of PTX with higher encapsulation efficiencies compared to hydrophilic drugs. Studies have shown the maximum cytostatic effect of PTX on solid ovarian and breast tumors occurs with paclitaxel concentrations of 1 μM (Gan et al., 1998; Millenbaugh et al., 1998), corresponding to approximately 0.9 μg of PTX/ml, suggesting that the drug loaded nanoshards located at the tumor will be powerful enough to cause cell damage.

The in vitro release profile of PTX from polymer UCA when triggered by ultrasound closely matched the uninsonated controls over the first week of release. This portion of the release profile is believed to be dominated by diffusion of drug through the polymer matrix (Shah et al., 1992). After 21 days, the release from drug loaded UCA triggered with ultrasound became significantly greater than the uninsonated controls (Fig. 8). This portion of the release profile is believed to be dominated by polymer degradation (Shah et al., 1992). The increased PTX release may be caused by the ultrasound triggered destruction of UCA resulting in polymer fragments as well as accelerated polymer degradation (Kost et al., 1989). As UCA cavitate in response to ultrasound (Ferrara, 2008), the high strain rate can fracture polymer chains, this polymer scission can reduce the polymer molecular weight and increase polymer degradation (Kuijpers et al., 2004). This enhanced polymer degradation has also been observed in contrast agents fabricated with poly

(lactic co glycolic acid) (El-Sherif et al., 2004). The release of PTX over the course of 1 month observed in this study demonstrates that the drug loaded particles that have the potential to accumulate within the tumor are capable of providing a sustained release of drug with similar release profiles observed in other polymer nanoparticles (Mu and Feng, 2003; Zhang et al., 2008; Patil et al., 2009). The advantage is that these nanoparticles are generated in situ, with greater likelihood of entering the tumor without the need to wait for the EPR effect.

Drug loaded UCA also showed an enhanced ability to pass through 400 nm pores when triggered with ultrasound (Fig. 9). This system is meant to model the leaky vasculature of a tumor and demonstrate the ability of the agent to be triggered by ultrasound to create fragments less than 400 nm, capable of passing through those pores. This system was limited by a lack of circulation which only exposed UCA within the focus of the transducer to sufficient energy to result in cavitation. The −6 dB focal zone of the transducer used was 3.19 mm while the diameter of the insert was 24 mm, resulting in only 1.8% of the total area being included in the focal zone in this stagnant system, however a significant increase in delivery through the 400 nm pores was still observed when UCA were triggered with ultrasound.

An in vitro cell viability assay showed that at tested concentration greater than 0.1 μg/ml, 18% PTX loaded UCA had significantly greater tumoricidal activity when first triggered with ultrasound compared to uninsonated controls. In vitro cell viability was not affected by unloaded polymer UCA at any concentrations tested indicating that all tumoricidal activity can be attributed to the PTX loaded within the agent.

In conclusion, a polymer UCA capable of cavitating and generating polymer fragments less than 400 nm when exposed to ultrasound has been loaded with both hydrophilic (DOX) and hydrophobic (PTX) drugs. While our DOX loaded platform has been plagued by lower drug payloads, the PTX loaded platform was shown to have a maximum payload twenty times greater than the hydrophilic drug loading. The agent showed significantly greater release of PTX over time when triggered with ultrasound compared to uninsonated controls ($p < 0.0374$). The agent also showed improved delivery through a polyester membrane with 400 nm pores when triggered with ultrasound compared to controls not exposed to ultrasound ($p < 0.0281$) as well as improved tumoricidal activity ($p < 0.01$).

Acknowledgements

This work was funded in part by the National Institute of Health (Grant HL-52901) and The Nanotechnology Institute of the Commonwealth of Pennsylvania's Ben Franklin Technology Development Authority through Ben Franklin Technology Partners of Southeastern PA.

Ultrasound imaging in vivo was performed with the expert assistance of Susan Schultz (University of Pennsylvania Hospital).

Confocal imaging was done with assistance from Steve Kemeny (Drexel MEM).

References

Bloch, S.H., Wan, M., Dayton, P.M., Ferrara, K.W., 2004. Optical observations of lipid and polymer-shelled ultrasound microbubble contrast agents. Appl. Phys. Lett. 84, 631–633.

Conlin, A.K., Seidman, A.D., 2007. Taxanes in breast cancer: an update. Curr. Oncol. Rep. 9, 22–30.

Dvorak, H.F., Brown, L.F., Detmar, M., Dvorak, A.M., 1995. Vascular permeability factor/vascular endothelial growth factor, microvascular hyperpermeability, and angiogenesis. Am. J. Pathol. 146, 1029–1039.

Eisenbrey, J.R., Huang, P., Hsu, J., Wheatley, M.A., 2009. Ultrasound triggered cell death in vitro with DOXorubicin loaded poly lactic-acid contrast agents. Ultrasonics 49, 628–633.

Eisenbrey, J.R., Burstein, O.M., Kambhampati, R., Forsberg, F., Liu, J.B., Wheatley, M.A., 2010a. Development and optimization of a doxorubicin loaded poly(lactic acid) contrast agent for ultrasound directed drug delivery. J. Control. Release 143, 38–44.

Eisenbrey, J.R., Soulen, M.C., Wheatley, M.A., 2010b. Delivery of encapsulated doxorubicin by ultrasound-mediated size reduction of drug-loaded polymer contrast agents. IEEE Trans. Biomed. Eng. 57, 24–28.

El-Sherif, D.M., Lathia, J.D., Le, N.T., Wheatley, M.A., 2004. Ultrasound degradation of novel polymer contrast agents. J. Biomed. Mater. Res. Part A 68, 71–78.

El-Sherif, D.M., Wheatley, M.A., 2003. Development of a novel method for synthesis of a polymeric ultrasound contrast agent. J. Biomed. Mater. Res. Part A 66, 347–355.

Fang, J., Nakamura, H., Maeda, H., 2011. The EPR effect: unique features of tumor blood vessels for drug delivery, factors involved, and limitations and augmentation of the effect. Adv. Drug Deliv. Rev. 63, 136–151.

Ferrara, K., Pollard, R., Borden, M., 2007. Ultrasound microbubble contrast agents: fundamentals and application to gene and drug delivery. Annu. Rev. Biomed. Eng. 9, 415–447.

Ferrara, K.W., 2008. Driving delivery vehicles with ultrasound. Adv. Drug Deliv. Rev. 60, 1097–1102.

Ferrara, K.W., Borden, M.A., Zhang, H., 2009. Lipid-shelled vehicles: engineering for ultrasound molecular imaging and drug delivery. Acc. Chem. Res. 42, 881–892.

Gan, Y., Wientjes, M.G., Lu, J., Au, J.L., 1998. Cytostatic and apoptotic effects of paclitaxel in human breast tumors. Cancer Chemother. Pharmacol. 42, 177–182.

Gaucher, G., Marchessault, R.H., Leroux, J.C., 2010. Polyester-based micelles and nanoparticles for the parenteral delivery of taxanes. J. Control. Release 143, 2–12.

Gelderblom, H., Verweij, J., Nooter, K., Sparreboom, A., 2001. Cremophor EL: the drawbacks and advantages of vehicle selection for drug formulation. Eur. J. Cancer 37, 1590–1598.

Gorce, J.M., Arditi, M., Schneider, M., 2000. Influence of bubble size distribution on the echogenicity of ultrasound contrast agents: a study of SonoVue. Invest. Radiol. 35, 661–671.

Green, M.R., Manikhas, G.M., Orlov, S., Afanasyev, B., Makhson, A.M., Bhar, P., Hawkins, M.J., 2006. Abraxane, a novel Cremophor-free, albumin-bound particle form of paclitaxel for the treatment of advanced non-small-cell lung cancer. Ann. Oncol. 17, 1263–1268.

Hamaguchi, T., Matsumura, Y., Suzuki, M., Shimizu, K., Goda, R., Nakamura, I., Nakatomi, I., Yokoyama, M., Kataoka, K., Kakizoe, T., 2005. NK105, a paclitaxel-incorporating micellar nanoparticle formulation, can extend in vivo antitumour activity and reduce the neurotoxicity of paclitaxel. Br. J. Cancer 92, 1240–1246.

Hobbs, S.K., Monsky, W.L., Yuan, F., Roberts, W.G., Griffith, L., Torchilin, V.P., Jain, R.K., 1998. Regulation of transport pathways in tumor vessels: role of tumor type and microenvironment. Proc. Natl. Acad. Sci. U. S. A. 95, 4607–4612.

Ibrahim, N.K., Desai, N., Legha, S., Soon-Shiong, P., Theriault, R.L., Rivera, E., Esmaeli, B., Ring, S.E., Bedikian, A., Hortobagyi, G.N., Ellerhorst, J.A., 2002. Phase I and pharmacokinetic study of ABI-007, a Cremophor-free, protein-stabilized, nanoparticle formulation of paclitaxel. Clin. Cancer Res. 8, 1038–1044.

Ishitobi, M., Shin, E., Kikkawa, N., 2001. Metastatic breast cancer with resistance to both anthracycline and docetaxel successfully treated with weekly paclitaxel. Int. J. Clin. Oncol. 6, 55–58.

Jemal, A., Siegel, R., Ward, E., Hao, Y., Xu, J., Murray, T., Thun, M.J., 2008. Cancer statistics, 2008. CA Cancer J. Clin. 58, 71–96.

Kang, B.K., Chon, S.K., Kim, S.H., Jeong, S.Y., Kim, M.S., Cho, S.H., Lee, H.B., Khang, G., 2004. Controlled release of paclitaxel from microemulsion containing PLGA and evaluation of anti-tumor activity in vitro and in vivo. Int. J. Pharm. 286, 147–156.

Klibanov, A.L., Shevchenko, T.I., Raju, B.I., Seip, R., Chin, C.T., 2010. Ultrasound-triggered release of materials entrapped in microbubble–liposome constructs: a tool for targeted drug delivery. J. Control. Release 148, 13–17.

Kong, G., Braun, R.D., Dewhirst, M.W., 2000. Hyperthermia enables tumor-specific nanoparticle delivery: effect of particle size. Cancer Res. 60, 4440–4445.

Kost, J., Leong, K., Langer, R., 1989. Ultrasound-enhanced polymer degradation and release of incorporated substances. Proc. Natl. Acad. Sci. U. S. A. 86, 7663–7666.

Kuijpers, W.M., Iedema, P.D., Kemmere, M.F., Keurentjes, T.J., 2004. The mechanism of cavitation-induced polymer scission; experimental and computational verification. Polymer 45, 6461–6467.

Lentacker, I., Geers, B., Demeester, J., De Smedt, S.C., Sanders, N.N., 2010. Design and evaluation of doxorubicin-containing microbubbles for ultrasound triggered doxorubicin delivery: cytotoxicicty and mechanisms involved. Mol. Ther. 18, 101–108.

Li, C., Wallace, S., 2008. Polymer-drug conjugates: recent development in clinical oncology. Adv. Drug Deliv. Rev. 60, 886–898.

Liggins, R.T., Hunter, W.L., Burt, H.M., 1997. Solid-state characterization of paclitaxel. J. Pharm. Sci. 86, 1458–1463.

Lum, A.F., Borden, M.A., Dayton, P.A., Kruse, D.E., Simon, S.I., Ferrara, K.W., 2006. Ultrasound radiation force enables targeted deposition of model drug carriers loaded on microbubbles. J. Control. Release 111, 128–134.

Maeda, H., Wu, J., Sawa, T., Matsumura, Y., Hori, K., 2000. Tumor vascular permeability and the EPR effect in macromolecular therapeutics: a review. J. Control. Release 65, 271–284.

Meijering, B.D., Juffermans, L.J., van Wamel, A., Henning, R.H., Zuhorn, I.S., Emmer, M., Versteilen, A.M., Paulus, W.J., van Gilst, W.H., Kooiman, K., de Jong, N., Musters, R.J., Deelman, L.E., Kamp, O., 2009. Ultrasound and microbubble-targeted delivery of macromolecules is regulated by induction of endocytosis and pore formation. Circ. Res. 104, 679–687.

Miele, E., Spinelli, G.P., Tomao, F., Tomao, S., 2009. Albumin-bound formulation of paclitaxel (Abraxane ABI-007) in the treatment of breast cancer. Int. J. Nanomed. 4, 99–105.
Millenbaugh, N.J., Gan, Y., Au, J.L., 1998. Cytostatic and apoptotic effects of paclitaxel in human ovarian tumors. Pharm. Res. 15, 122–127.
Mu, L., Feng, S.S., 2003. A novel controlled release formulation for the anticancer drug paclitaxel (Taxol): PLGA nanoparticles containing vitamin E TPGS. J. Control. Release 86, 33–48.
Patil, Y., Sadhukha, T., Ma, L., Panyam, J., 2009. Nanoparticle-mediated simultaneous and targeted delivery of paclitaxel and tariquidar overcomes tumor drug resistance. J. Control. Release 136, 21–29.
Panyam, J., Labhasetwar, V., 2003. Biodegradable nanoparticles for drug and gene delivery to cells and tissue. Adv. Drug Deliv. Rev. 55, 329–347.
Price, R.J., Skyba, D.M., Kaul, S., Skalak, T.C., 1998. Delivery of colloidal particles and red blood cells to tissue through microvessel ruptures created by targeted microbubble destruction with ultrasound. Circulation 98, 1264–1267.
Rosenblum, M.D., Shivers, R.R., 2000. 'Rings' of F-actin form around the nucleus in cultured human MCF7 adenocarcinoma cells upon exposure to both taxol and taxotere. Comp. Biochem. Physiol. C Toxicol. Pharmacol. 125, 121–131.
Rowinsky, E.K., Donehower, R.C., 1995. Paclitaxel (taxol). N. Engl. J. Med. 332, 1004–1014.
Shah, S.S., Cha, Y., Pitt, C.G., 1992. Poly(glycolic acid-co-DL-lactic acid): diffusion or degradation controlled drug delivery? J. Control. Release 18, 261–270.
Singla, A.K., Garg, A., Aggarwal, D., 2002. Paclitaxel and its formulations. Int. J. Pharm. 235, 179–192.
Tartis, M.S., McCallan, J., Lum, A.F., LaBell, R., Stieger, S.M., Matsunaga, T.O., Ferrara, K.W., 2006. Therapeutic effects of paclitaxel-containing ultrasound contrast agents. Ultrasound Med. Biol. 32, 1771–1780.
Thigpen, J.T., Blessing, J.A., Ball, H., Hummel, S.J., Barrett, R.J., 1994. Phase II trial of paclitaxel in patients with progressive ovarian carcinoma after platinum-based chemotherapy: a Gynecologic Oncology Group study. J. Clin. Oncol. 12, 1748–1753.
van Wamel, A., Bouakaz, A., Versluis, M., de Jong, N., 2004. Micromanipulation of endothelial cells: ultrasound–microbubble–cell interaction. Ultrasound Med. Biol. 30, 1255–1258.
van Wamel, A., Kooiman, K., Harteveld, M., Emmer, M., ten Cate, F.J., Versluis, M., de Jong, N., 2006. Vibrating microbubbles poking individual cells: drug transfer into cells via sonoporation. J. Control. Release 112, 149–155.
Weiss, R.B., Donehower, R.C., Wiernik, P.H., Ohnuma, T., Gralla, R.J., Trump, D.L., Baker Jr., J.R., Van Echo, D.A., Von Hoff, D.D., Leyland-Jones, B., 1990. Hypersensitivity reactions from taxol. J. Clin. Oncol. 8, 1263–1268.
Xie, J., Wang, C.H., 2005. Self-assembled biodegradable nanoparticles developed by direct dialysis for the delivery of paclitaxel. Pharm. Res. 22, 2079–2090.
Yeung, T.K., Germond, C., Chen, X., Wang, Z., 1999. The mode of action of taxol: apoptosis at low concentration and necrosis at high concentration. Biochem. Biophys. Res. Commun. 263, 398–404.
Zhang, Z., Lee, S.H., Gan, C.W., Feng, S.S., 2008. In vitro and in vivo investigation on PLA–TPGS nanoparticles for controlled and sustained small molecule chemotherapy. Pharm. Res. 25, 1925–1935.